

Modeling Plumes from Cryogenic Hydrogen Sources

Ethan Hecht

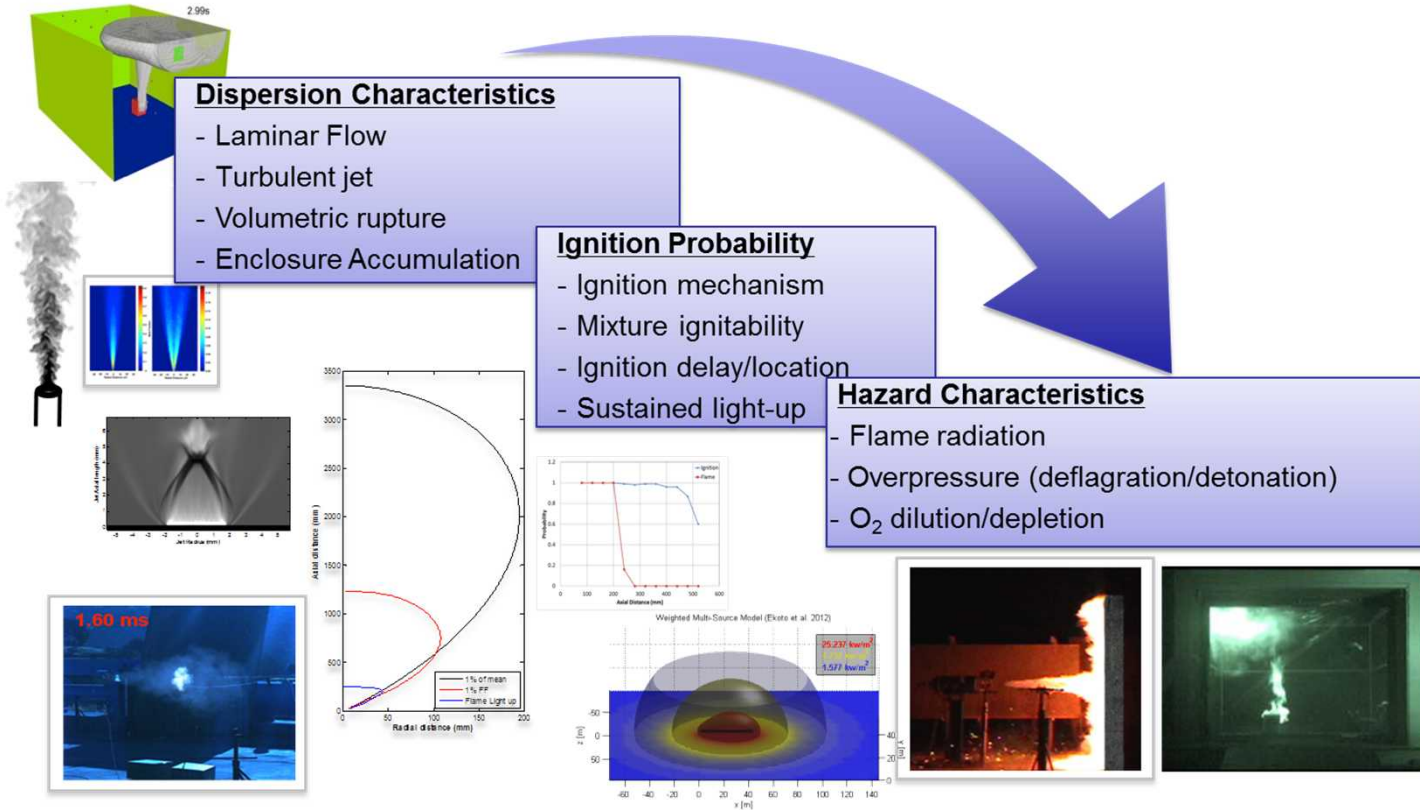
Isaac Ekoto

Chris San Marchi



Sandia National Laboratories is a multi-program laboratory managed and operated by Sandia Corporation, a wholly owned subsidiary of Lockheed Martin Corporation, for the U.S. Department of Energy's National Nuclear Security Administration under contract DE-AC04-94AL85000. SAND NO. 2011-XXXXP

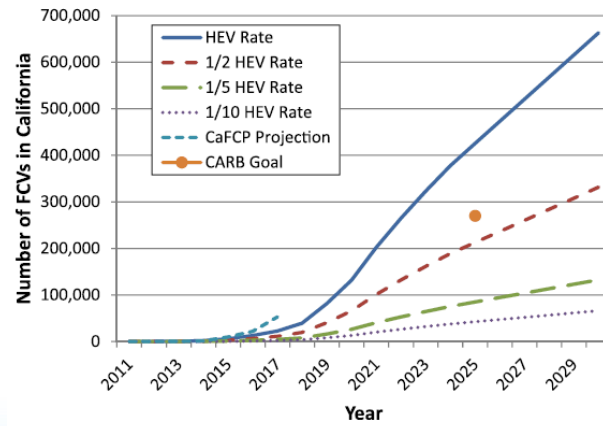
Quantitative risk assessment requires validated behavior models for different scenarios



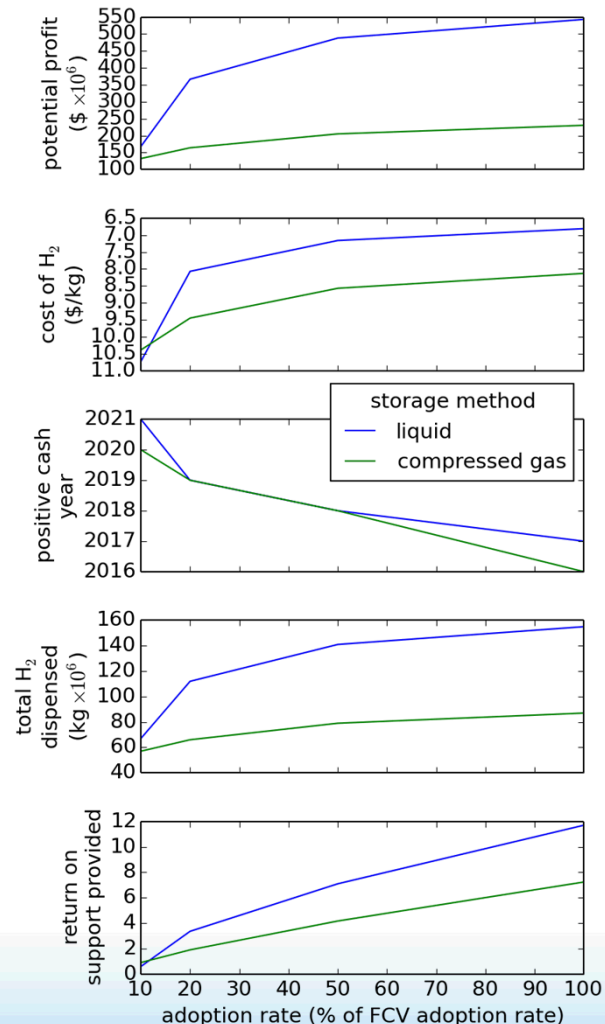
$$Risk \propto \sum_{i,j,k} P(\text{Release}_i) P(\text{Ignition}_j | \text{Release}_i) P(\text{Hazard}_k | \text{Ignition}_j \cap \text{Release}_i) P(\text{Harm} | \text{Hazard}_k)$$

Terms in red obtained from physical behavior models, while terms in black are based on scenario frequencies and probit harm models

Economic analyses for a proposed CA network of 68 H₂ fuel stations suggests LH₂ has long-term benefit over GH₂



Brown et al., IJHE, 2013



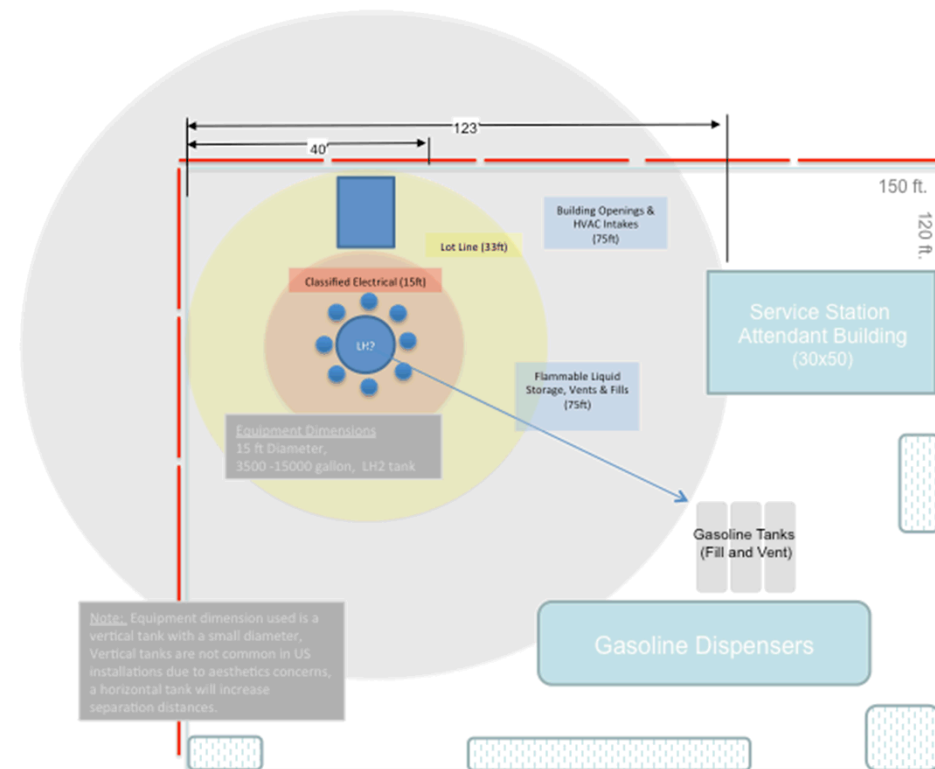
Analysis does not consider feasibility based on safety requirements.

Survey of California Energy Commission preferred stations suggest LH2 separation distances would be prohibitive

Separation Distances (NFPA 2-2011) and Areas required for two station concepts (critical distances and areas emphasized)		
Fueling System Description	GH2	LH2
GH2: 12,500psi storage, 100kg, 0.4"ID tubing with a barrier wall LH2: 3500-15000 gallon (910-1300kg) with barrier wall and insulation		
Lot lines (ft)	24	33
Public Streets, Alleys (ft)	24	33
Parking (public assembly) (ft)	13	75
Buildings (sprinkled, fire rated) (ft)	10	5
Building Openings or air intakes (ft)	24	75
Flammable and Combustible liquid storage, vents or fill ports (ft)	10	50
Parking from fill connections on bulk storage (ft)	13	25
Class 1 Div. 2 area diameter (ft)	15	15
Max Bulk Storage Dimensions with Sep. Distances (ft)	78	123
Min Bulk Storage Dimension with Sep. Distances (ft)	68	123
Max Bulk Storage Equipment Dimension with lot lines (ft)	54	40
Min Bulk Storage Equipment Dimension with lot lines (ft)	49	40
Reference Bulk Storage Equipment Area with lot lines (sqft)	2646	1600
Reference Storage Area with Sep. Distances (sqft)	5304	15129
Note: Add 5 feet for vehicle protection on vehicle facing sides of equipment		

Harris, SAND-2014-XXXX

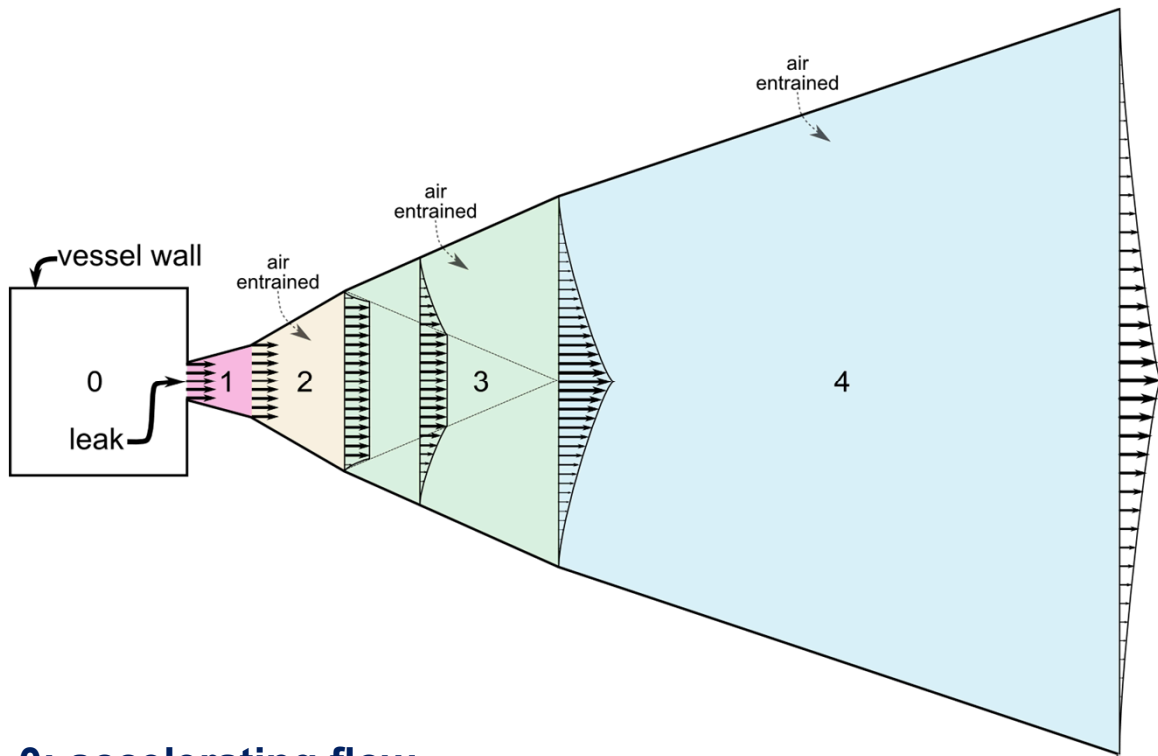
Of 70 stations surveyed (out of 343), none met the NFPA 2 Ch. 6 separation distance requirements.



Improved LH2 modeling needed to reduce separation distances and increase the viability of risk informed certification (e.g., NFPA 2 Ch. 5)

SNL conceptual model for LH₂ releases developed in 2009

- Steady-state
- 1-dimensional (along streamline coordinate)

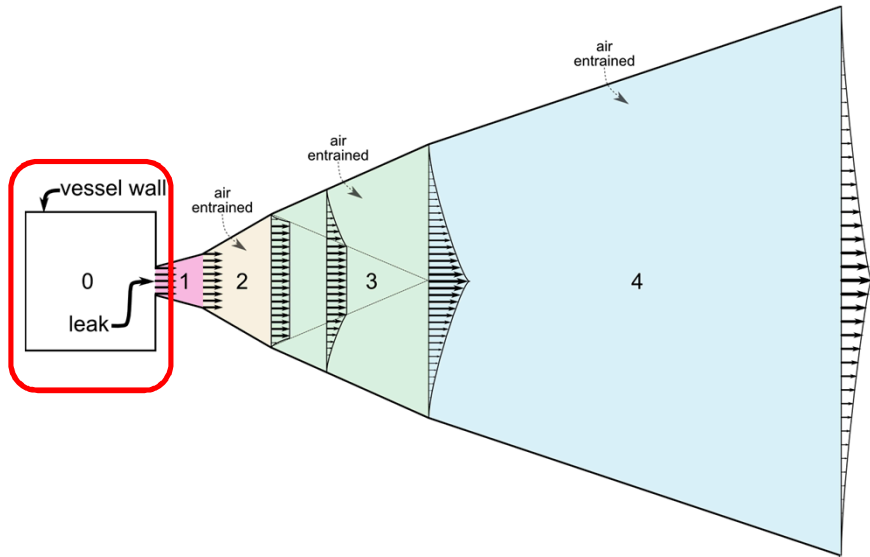


- Zone 0: accelerating flow
- Zone 1: underexpanded jet
- Zone 2: initial entrainment and heating
- Zone 3: flow establishment
- Zone 4: self-similar, established flow

Winters, SAND Report 2009-0035
Winters & Houf, IJHE, 2011
Houf & Winters, IJHE, 2013

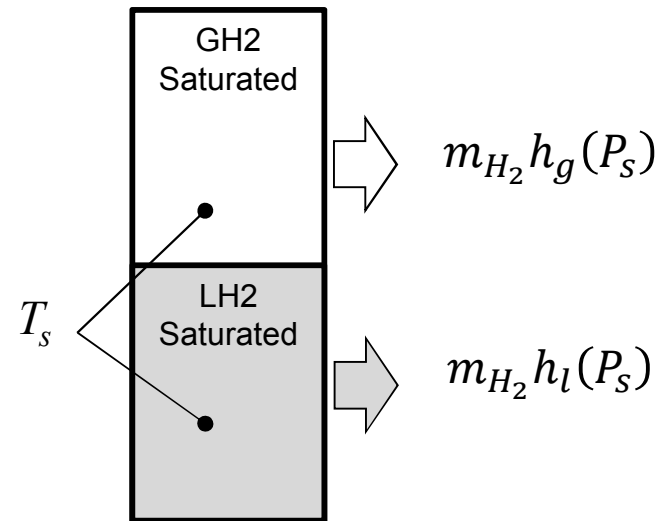
SNL Network Flow Analysis Code (NETFLOW) used to model internal conditions in piping, valve, and tanks

Accelerating flow (leak) develops from saturated storage conditions

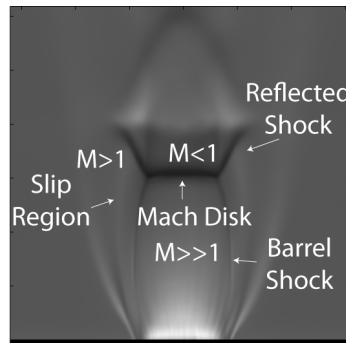
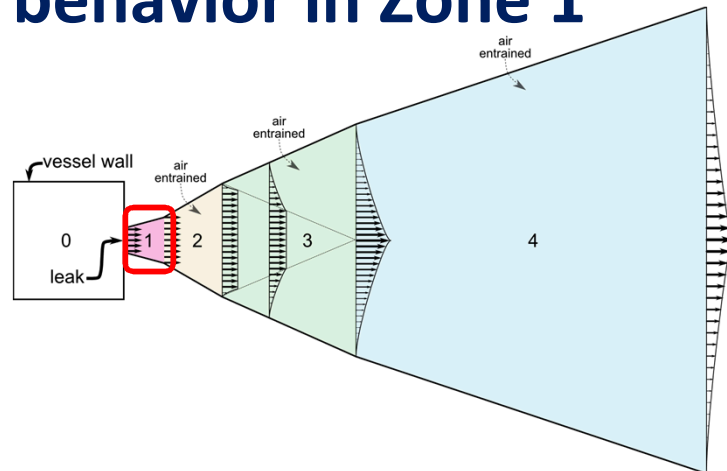


- conserved enthalpy from the gas or liquid space.

Winters, SAND 2001-8422



Pseudo source models are used to account for choked flow behavior in Zone 1



Source Model	$d^* [mm]$
Birch et al. (1984)	0.947
Ewan & Moodie (1986)	0.993
Birch et al. (1987)	0.790
Harstad & Bellan (2006)	1.440
Molkov (2008)	0.993
SNL Data (2011)	0.867

*All models updated w/ Able-Noble EOS

Ruggles & Ekoto, *IJHE*, 2012

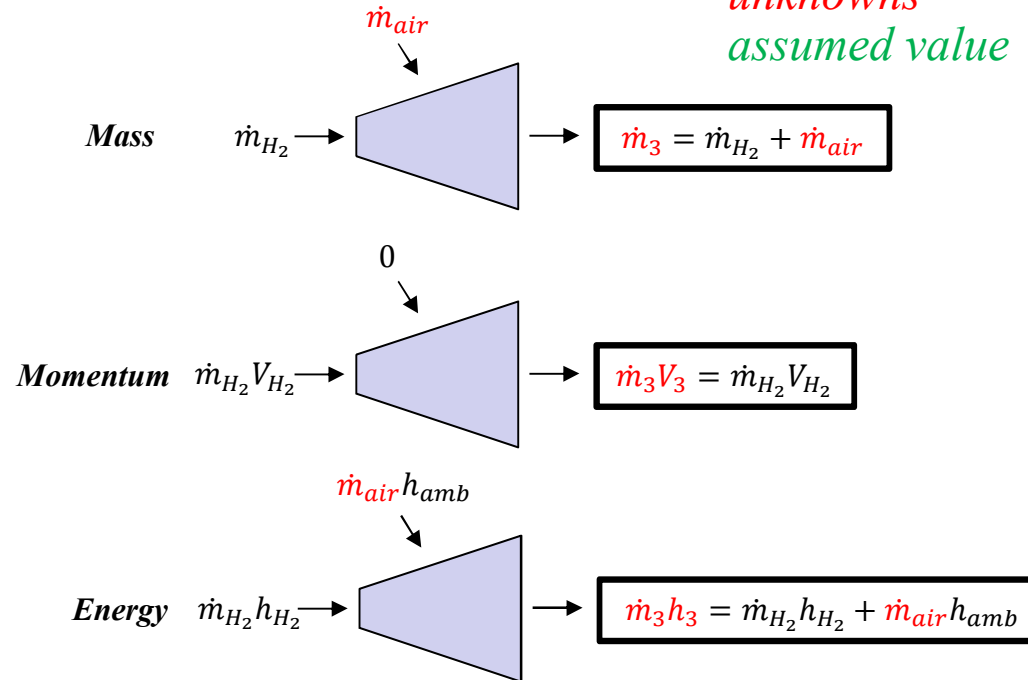
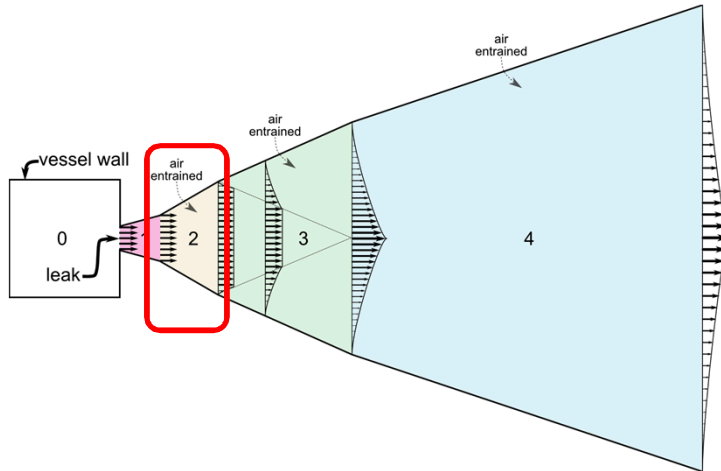
Neglects Mach Disk
(i.e., fully supersonic)

Assumes **all** flow goes through
Mach disk (i.e., fully subsonic)

Reality is that fluid is split
between the slip and
Mach disk regions

Ongoing work to develop validated two-zone source model that accounts for the fluid split ratio between the slip region & Mach disk regions

Plug flow assumption invoked for Zone 2



Winters, SAND Report 2009-0035

State modeling by NIST H₂ EOS:

$$h_3 = f(Y_{H_2,3}, p_{amb}, T_3)$$

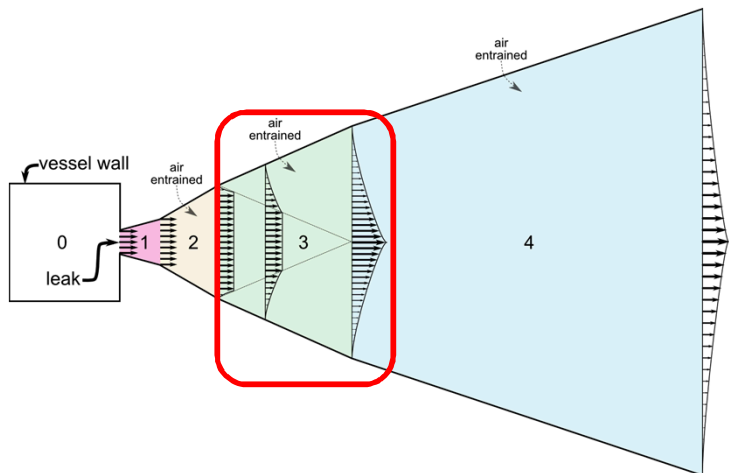
Species conservation used to close system of equations:

$$\dot{m}_{air} = \dot{m}_{H_2} \frac{1 - Y_{H_2,3}}{Y_{H_2,3}}$$

Turbulent jet entrainment rate used to estimate zone length:

$$E_{mom} \equiv \frac{1}{\rho_{amb}} \frac{d\dot{m}}{dS} \approx \frac{1}{\rho_{amb}} \frac{\dot{m}_{air}}{S_3} \Rightarrow S_3 = \frac{\dot{m}_{air}}{E_{mom} \rho_{amb}}, \text{ where } E_{mom} = \alpha_m \left(\frac{\pi D_{H_2}^2}{4} \frac{\rho_{H_2} V_{H_2}^2}{\rho_{amb}} \right)^{\frac{1}{2}}$$

Zone 3 treated as discrete region w/ boundary conditions specified from self-similar profiles at Zone 4



unknowns
assumed value

$$V_{CL,4} = V_3$$

Mass

$$\rho_3 \frac{D_3^2}{4} = B_4^2 \left[\rho_{amb} - \frac{\lambda^2}{\lambda^2 + 1} (\rho_{amb} - \rho_{CL,4}) \right]$$

Momentum

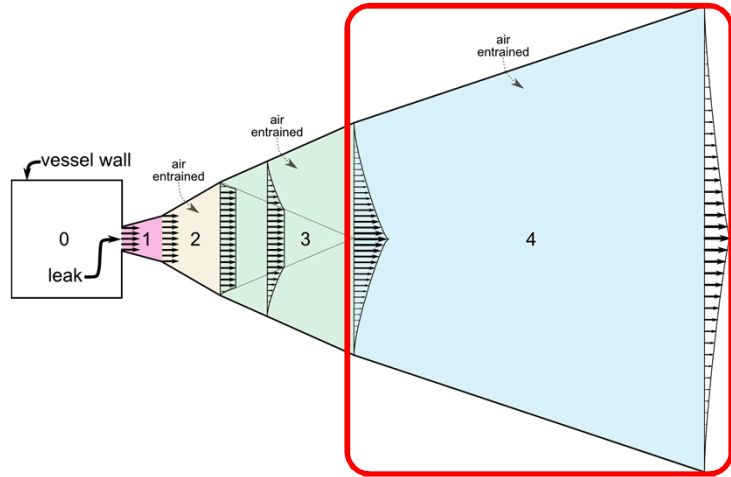
$$(\rho_{amb} - \rho_3) \frac{D_3^2}{4} = B_4^2 \left[\frac{\rho_{amb}}{2} - \frac{\lambda^2}{2\lambda^2 + 1} (\rho_{amb} - \rho_{CL,4}) \right]$$

S_3

S_4

Winters, SAND Report 2009-0035

Zone 4 modeled with previous SNL 1D integral jet/plume models that invoke self-similarity – FY08



Entrainment due to buoyancy & momentum

F_{rL} : Jet Froude length

α_b : Buoyancy entrainment coefficient

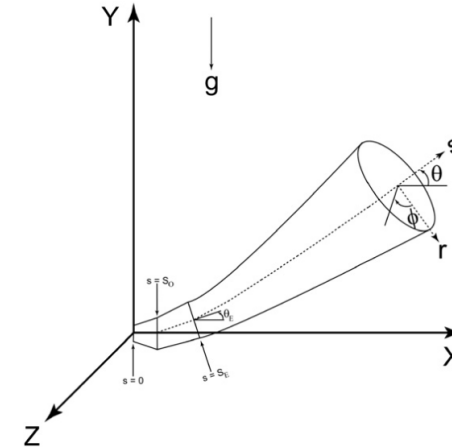
α_m : Momentum entrainment coefficient

g : Gravity constant

$$E_{buoy} = \frac{\alpha_b}{F_{rL}} (2\pi V_{CL} B) \sin \theta$$

$$E_{mom} = \alpha_m \left(\frac{\pi D^2}{4} \frac{\rho V^2}{\rho_{amb}} \right)^{\frac{1}{2}}$$

$$F_{rL} = \frac{V_{CL}^2 \rho_{exit}}{g B (\rho_{amb} - \rho_{CL})}$$



$$\text{Mass} \quad \frac{\partial}{\partial S} \int_0^{2\pi} \int_0^{\infty} \rho V r dr d\phi = \rho_{amb} E$$

$$\text{x-Mom} \quad \frac{\partial}{\partial S} \int_0^{2\pi} \int_0^{\infty} \rho V^2 \cos \theta r dr d\phi = 0$$

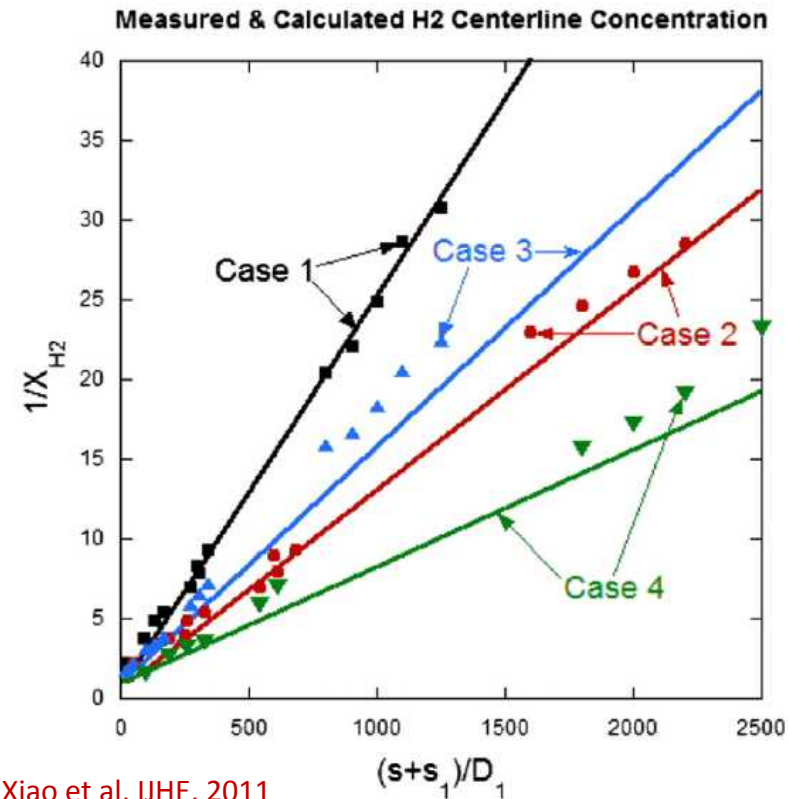
$$\text{y-Mom} \quad \frac{\partial}{\partial S} \int_0^{2\pi} \int_0^{\infty} \rho V^2 \sin \theta r dr d\phi = \int_0^{2\pi} \int_0^{\infty} (\rho_{amb} - \rho) g r dr d\phi$$

$$\text{Species} \quad \frac{\partial}{\partial S} \int_0^{2\pi} \int_0^{\infty} \rho V Y r dr d\phi = 0$$

$$\text{Energy} \quad \frac{\partial}{\partial S} \int_0^{2\pi} \int_0^{\infty} \rho V (h - h_{amb}) r dr d\phi = 0$$

Model results compare favorably to experiments from Karlsruhe Institute of Technology

Case	Reservoir pressure [MPa]	Reservoir temperature [K]	Leak diameter [mm]
1	1.7	298	2
2	6.85	298	1
3	0.825	80	2
4	3.2	80	1



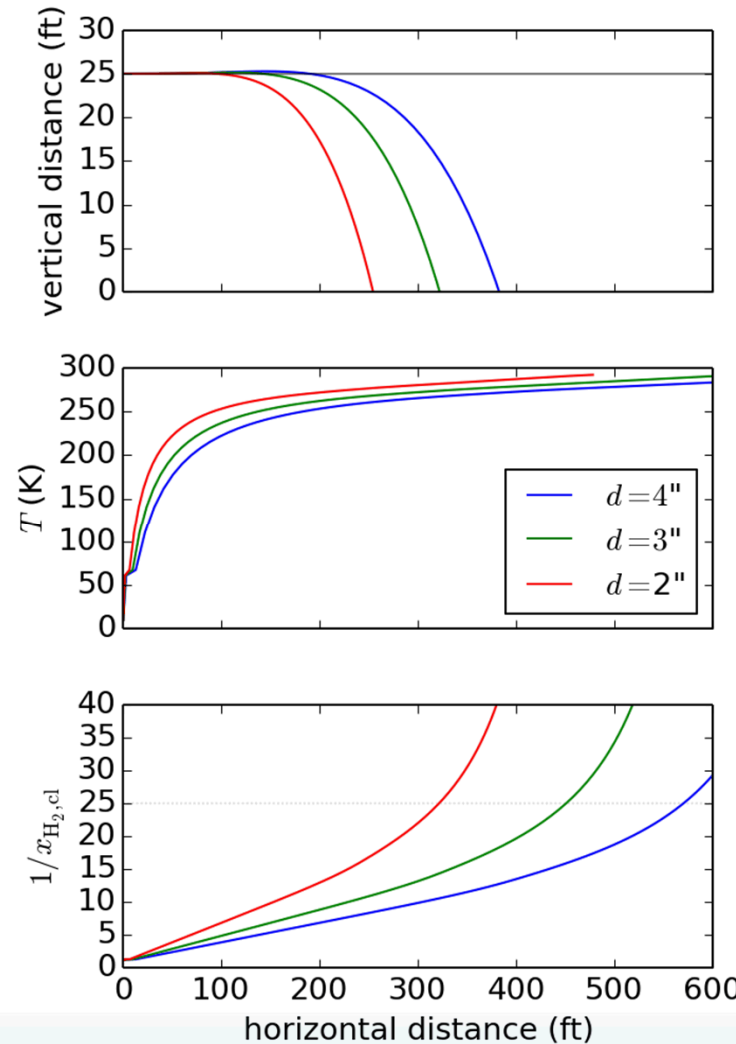
Xiao et al, IJHE, 2011

Houf & Winters, IJHE, 2013

However, no well-controlled validation data is available at lower temperatures where multi-phase flows are expected (i.e., T < 77 K)

Regardless of leak size, heavy jet falls towards the ground

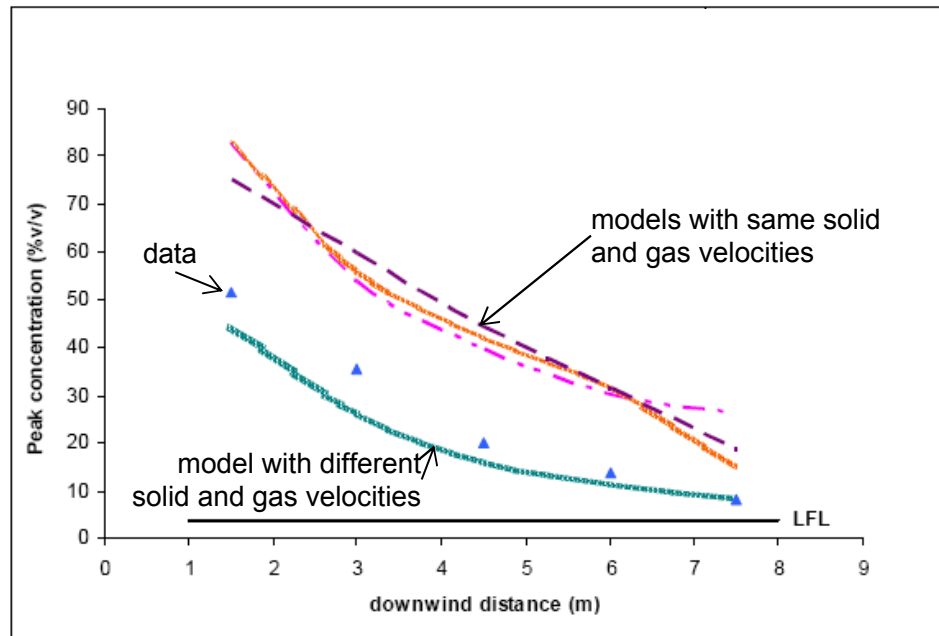
- Storage pressure = 180 psi
- Release (saturation) temperature = 20 K
- Release angle = 0°
- Release height = 25 ft



Clear need to develop jet-impingement model to account for spread along the ground

Multi-phase behavior is important—particularly for high-humidity conditions

Liquid and vapor phases have different velocities due to density differences — slip models have captured these effects in CFD simulations.



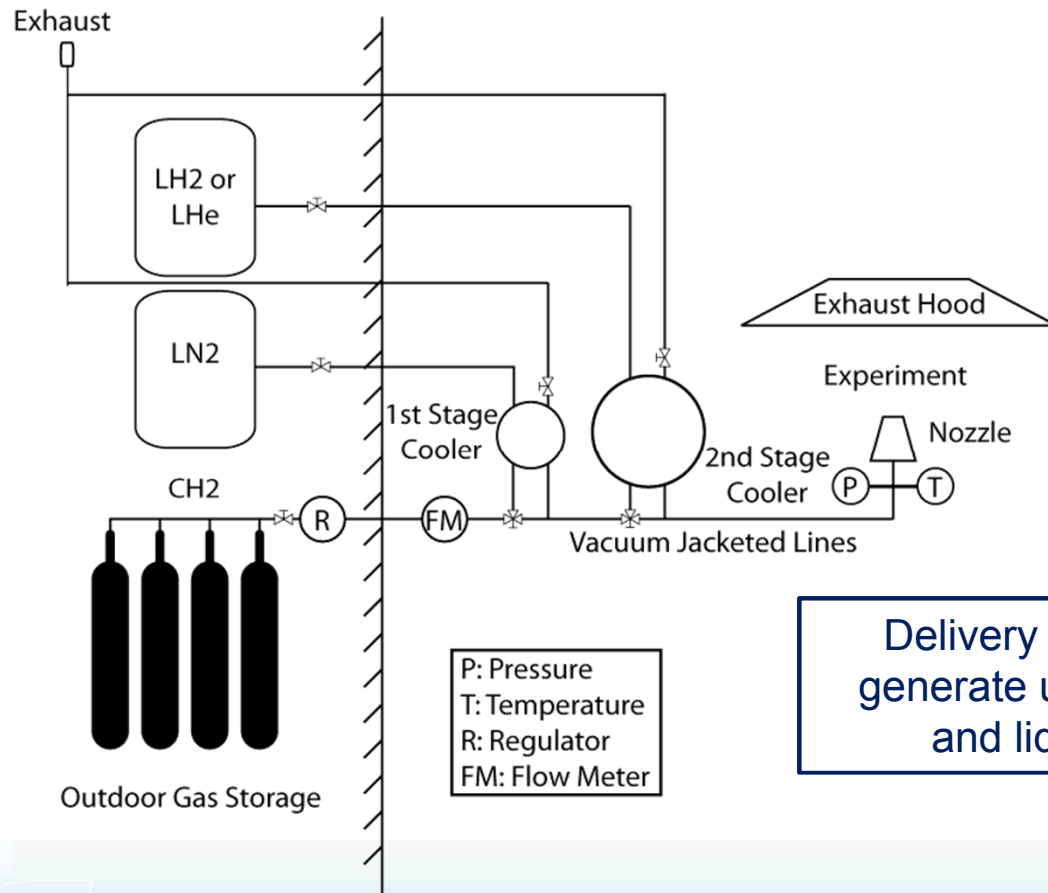
HSL Measurements: Sample probes
Hooker et al, ICHS, 2011

ADREA-HF CFD Simulations
Giannissi et al, ICHS, 2013

Substantial differences in model results suggest 2-phase effects cannot be neglected for LH₂ releases

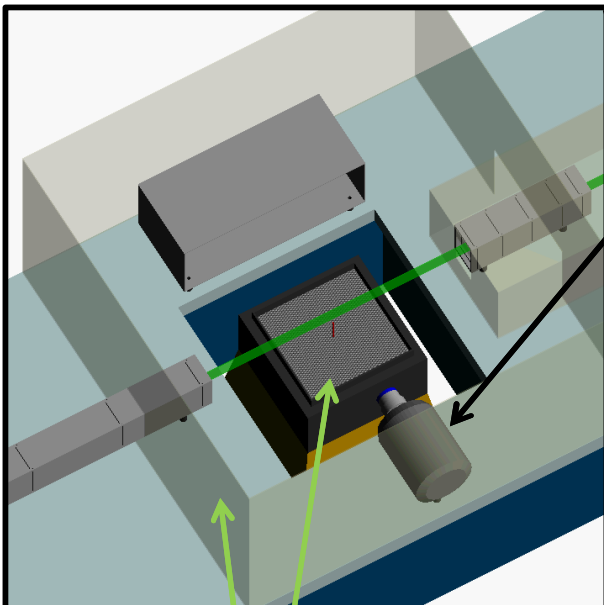
Experiments had poor control of release and environmental boundary conditions, which are needed for suitable benchmark data

Proposal is to build an LH₂ delivery system that can be integrated w/ existing SNL laboratory infrastructure



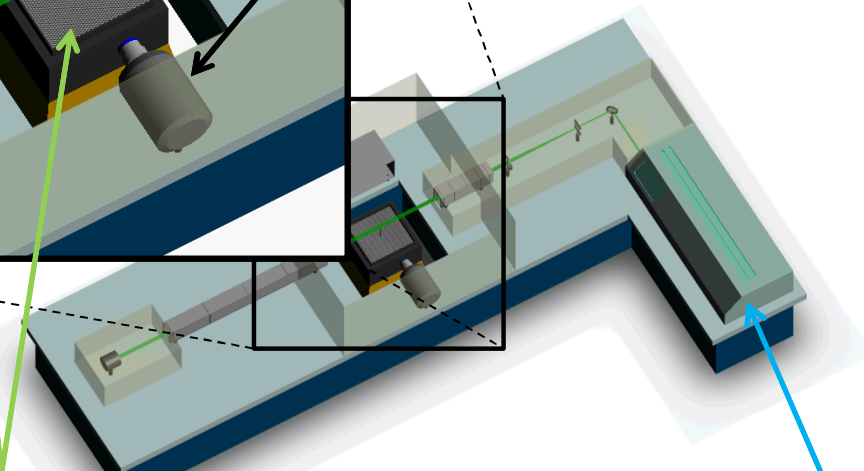
System design, construction, & verification ~12 months, w/ another 6-12 months for measurements – system cost ~\$150K plus labor

Scalar field to be measured via Rayleigh scatter imaging in established flow zone to validate LH2 release model



PIXIS 400B low noise CCD Camera

- 2 x 2 binning for high signal-to-noise (~400:1)
- Multiple interrogation regions to image full jet
- Multiple images for converged statistics



Air co-flow & barriers to minimize impact of room currents

Nd:YAG injection seeded laser (1 J/pulse @ 532 nm)



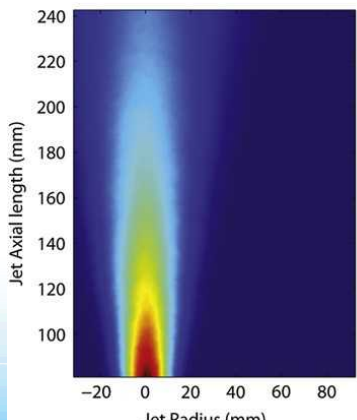
Opportunity for additional upstream measurements using complementary Raman diagnostics in an adjacent lab

Quantitative measurement w/ good accuracy

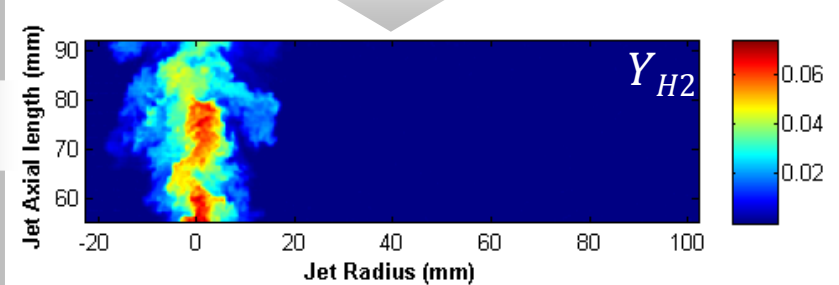
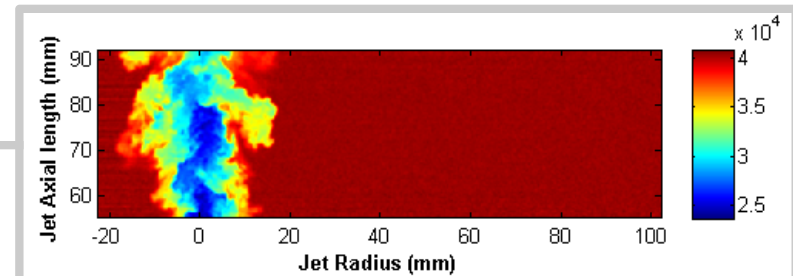
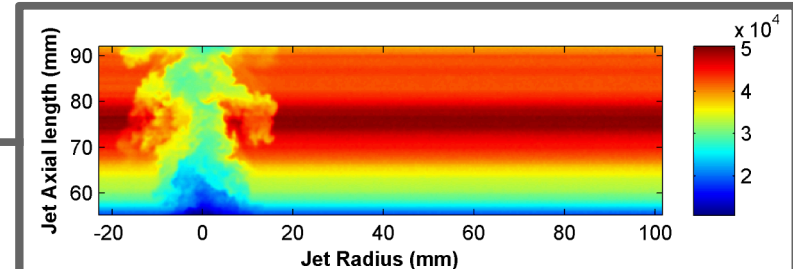
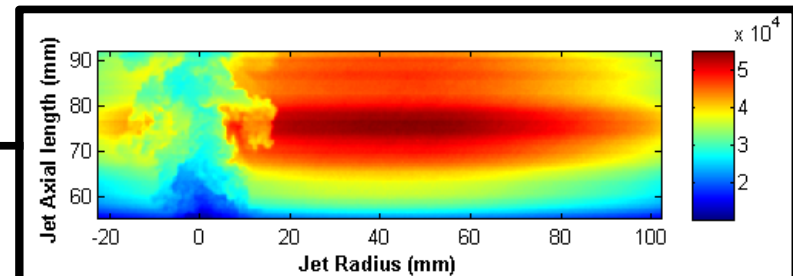
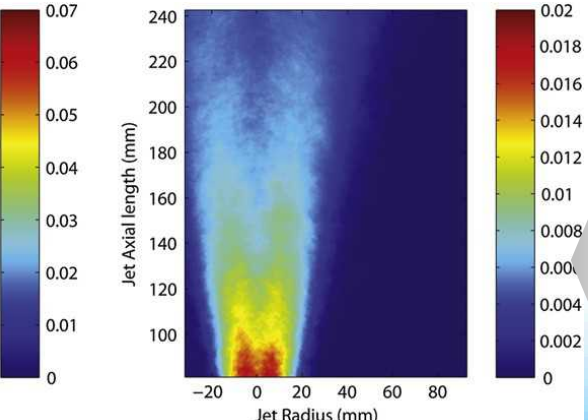
- R : Raw image
- E_B : Electronic bias
- B_G : Background luminosity
- p_F : Laser power fluctuation
- O_R : Camera/lens optical response
- S_B : Background scatter
- S_t : Laser sheet profile variation
- I : Corrected intensity

$$R = p_F \cdot O_R \cdot (I \cdot S_t + S_B) + E_B + B_G$$

Mean mole fraction



RMS Error



Backup Slides

Compressed gas release hazard example: overpressure

$$\Delta p = p_0 \left\{ \left[\frac{V_T + V_{H2}}{V_T} \frac{V_T + V_{stoich}(\sigma - 1)}{V_T} \right]^\gamma - 1 \right\}$$

Bauwens & Dorofeev, ICHS, 2013.

p_0 : Ambient pressure
 V_T : Facility volume
 V_{H2} : Expanded volume of pure H₂
 V_{stoich} : Stoichiometric consumed H₂ volume
 σ : Stoichiometric H₂ expansion ratio
 γ : Air specific heat ratio (1.4)

H2 indoor refueling experiments & modeling

Ekoto et al. IJHE 2012

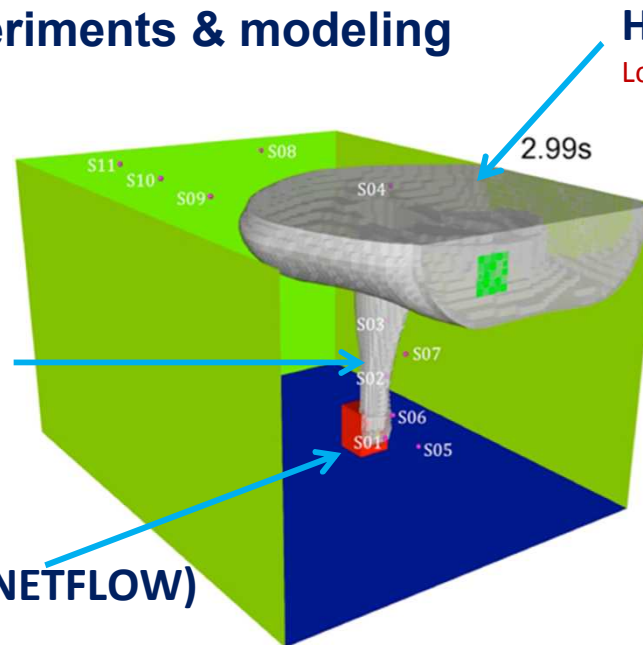
Houf et al. IJHE 2013

SNL H2 Jet/Plume Model

Houf & Schefer, IJHE 2008

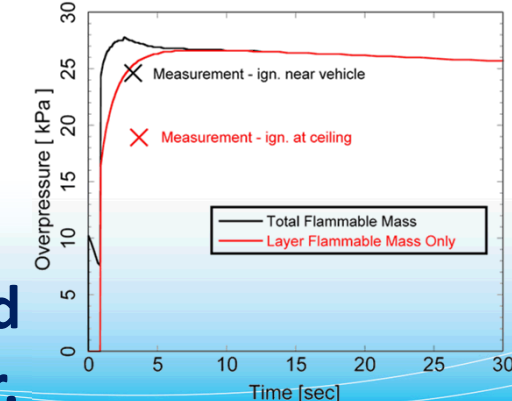
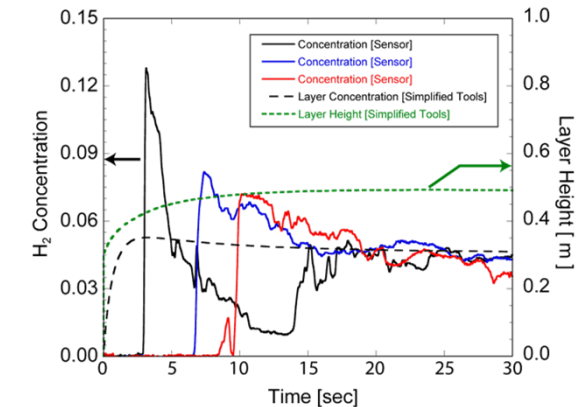
SNL Network Flow Model (NETFLOW)

Winters, SAND 2001-8422



H2 Layer Accumulation Model

Lowesmith et al. IJHE 2009



Exercise demonstrates how previous reduced-order model development work can be leveraged to quickly & accurately predict complex behavior.

Jet Flame Radiation Modeling

Three jet flame radiative heat flux model categories:

Single Point Source (SPS) models

Flame shape:

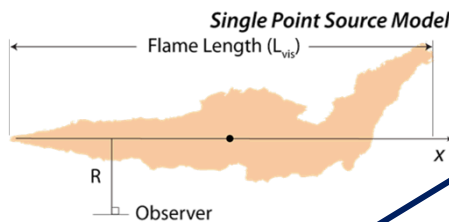
- Non-dimensional radiant power to estimate radiant load distribution

Radiant fraction models:

- Empirical function: temperature, composition, release rate, soot, residence time, heat release

Sivathanu & Gore, Combust Flame, 1993

Molina et al., Proc Combust Inst, 2007



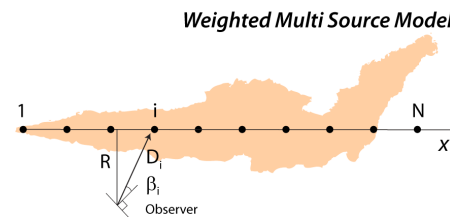
Flame shape:

- Weighted source emitters along flame centerline

De-Faveri et al., Hydrocarbon Processing, 1985

Hankinson & Lowesmith, Combust Flame, 2012

Multi Source Models (MSM)



Radiant fraction models:

- Same as SPS models

Single Surface models

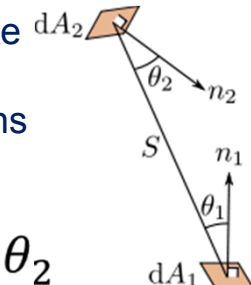
Flame shape:

- Assumed flame shape (e.g., cone) w/ empirically tuned radiating surface
- Geometric View Factors to calculate radiation transfer
- Empirical wind/buoyancy corrections

Chamberlain, Chem Eng Res Des, 1987

Johnson et al., Process Safety Environ Prot, 1994

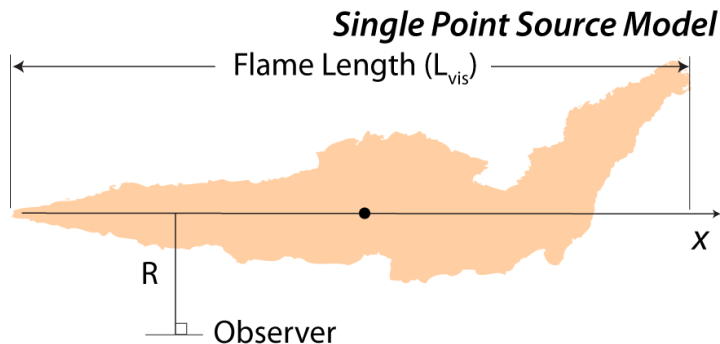
$$VF_{1 \rightarrow 2} = \frac{\cos \theta_1 \cos \theta_2}{\pi S^2}$$



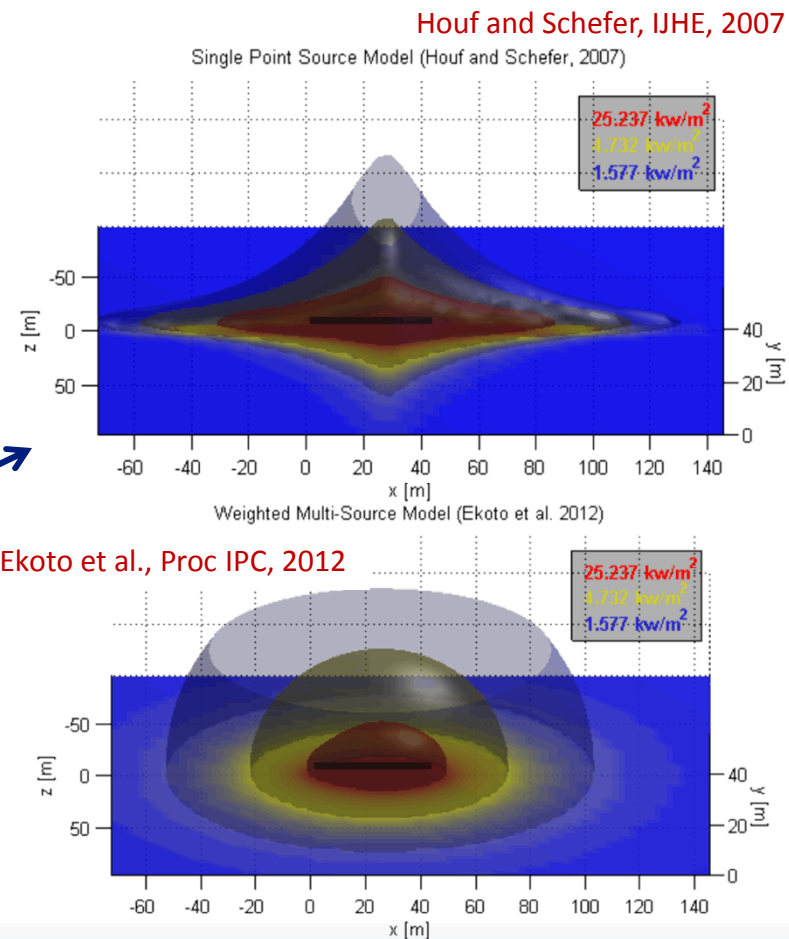
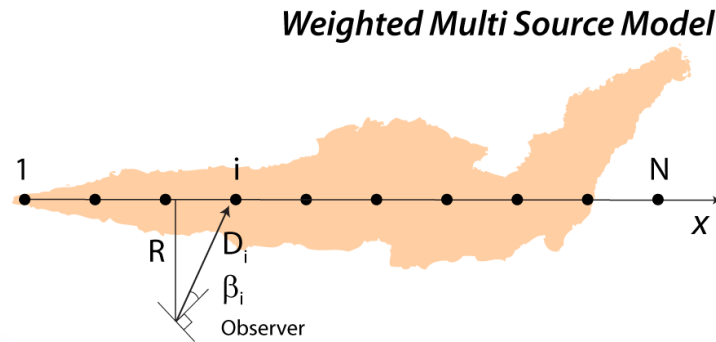
Previous Accomplishments

Large-scale flame data supplied by Air Products and Chemicals Inc.

d_j [mm]	[kg/s]	L_{vis} [m]	p_0 [barg]	T_0 [K]	T_{amb} [K]	p_{amb} [bar]
50.8	7.4	48.5	62.1	288	280	1.01



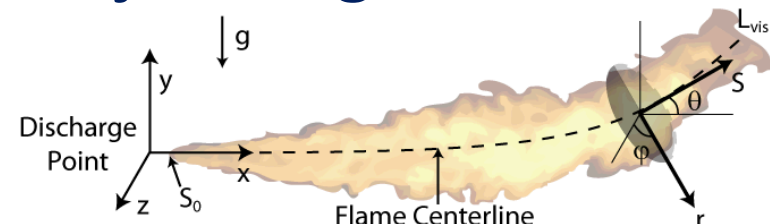
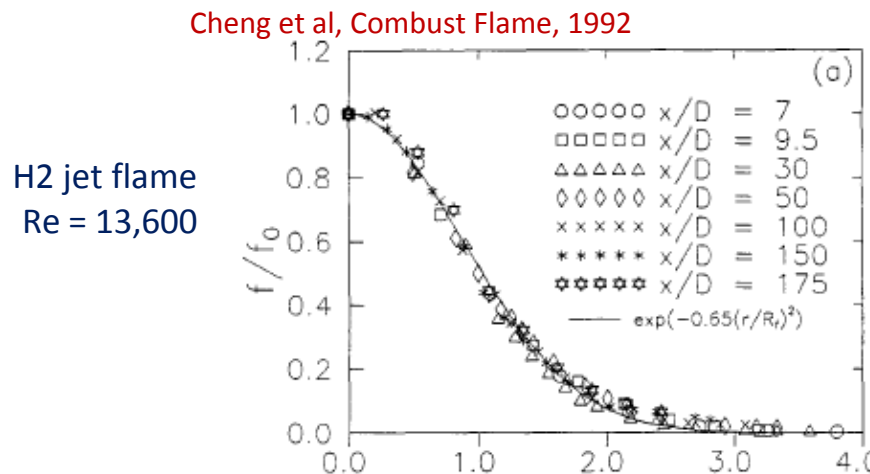
Old model used to inform NFPA 2/55



Improved radiative heat flux boundaries for more accurate harm & improved recommendations for reduced separation distances.

- Model can be improved with a better prediction of flame trajectory to better

Flame integral model is similar to 1D jet integral models



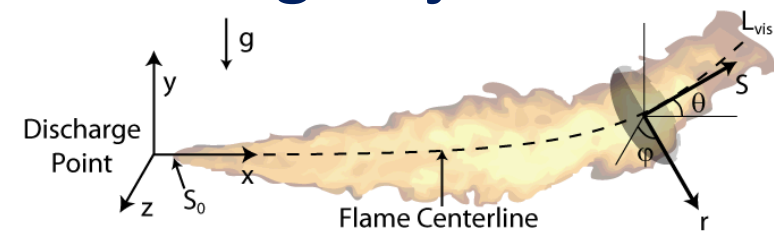
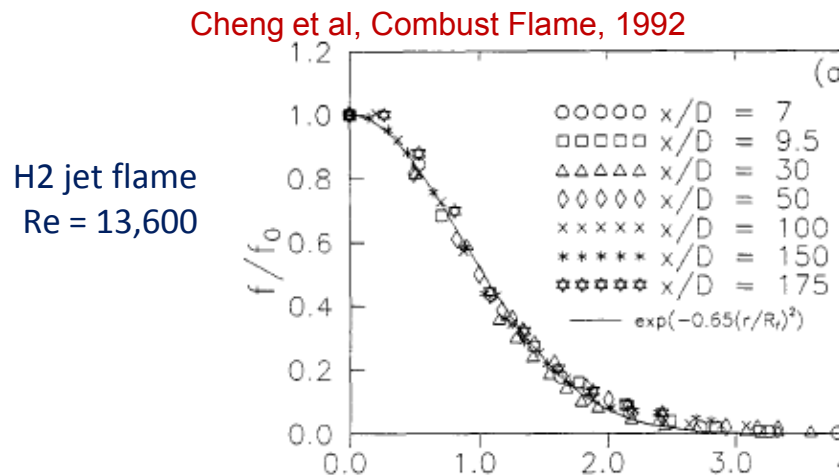
Species are no longer conserved & excess state variable profiles depend on the degree of chemical reaction

Self-similar, Gaussian mixture fraction profiles observed at all radials throughout the flame

$$\underbrace{\frac{\partial}{\partial S} \int_0^{2\pi} \int_0^{\infty} \rho V Y r dr d\phi}_{\text{H}_2 \text{ Species Conservation}} \text{ replaced by, } \underbrace{\frac{d}{dS} \int_0^{2\pi} \int_0^{\infty} \rho V f r dr d\phi = 0}_{\text{Mixture Fraction Conservation}} \text{ where, } f = Y_{H_2} + Y_{H_2O} \frac{MW_{H_2}}{MW_{H_2O}}$$

Mixture fraction is a conserved scalar that can replace H₂ mass fraction in the conservation equations

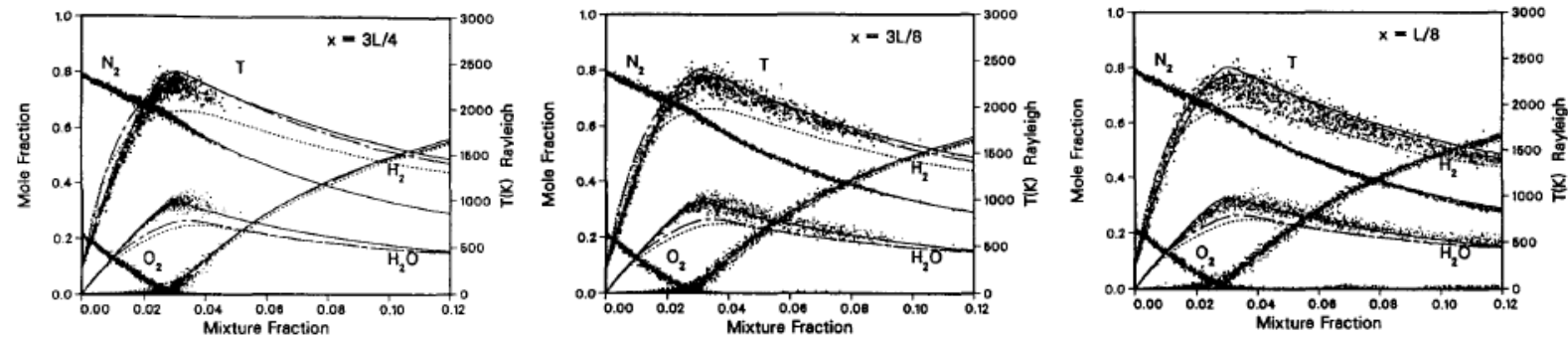
Flame integral model is similar to existing 1D jet models



Species are no longer conserved & **excess state variable profiles depend on the degree of chemical reaction**

Self-similar, Gaussian mixture fraction profiles observed at all radials throughout the flame

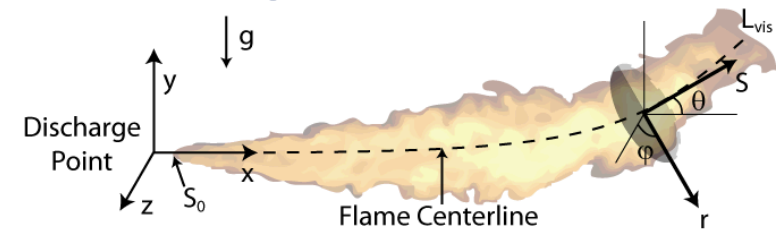
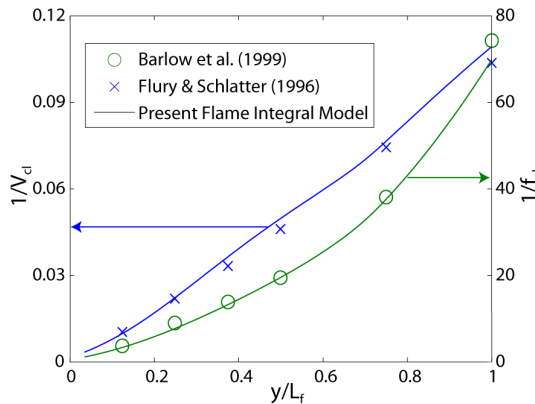
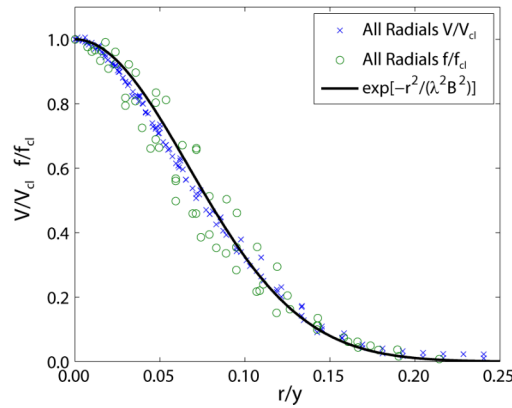
Barlow & Carter, Combust Flame, 1994



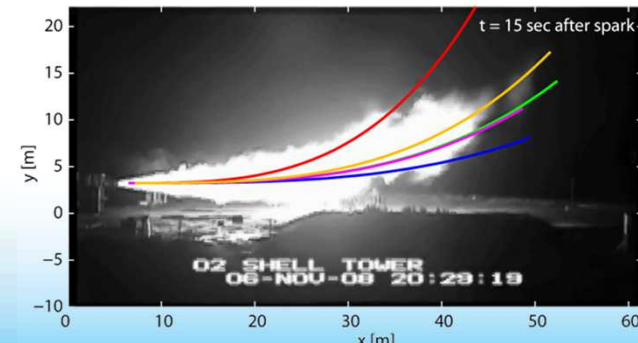
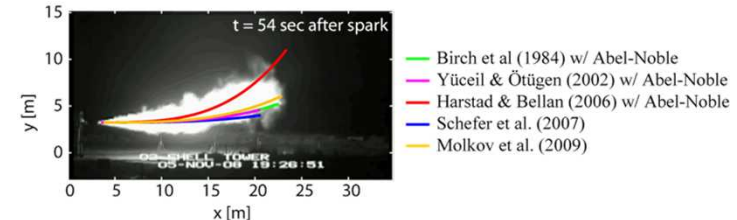
H₂ jet flame; Re = 10,000

Composition/Temperature at most points was close to equilibrium solution — energy conservation can be neglected if equilibrium kinetics are assumed

Model performs well when applied to large-scale flames



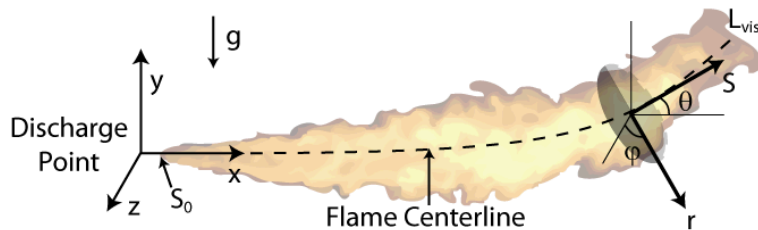
Entrainment rate coefficients & jet spreading ratios adjusted to match experimental data



Centerline trajectory results highly dependent on choked source model

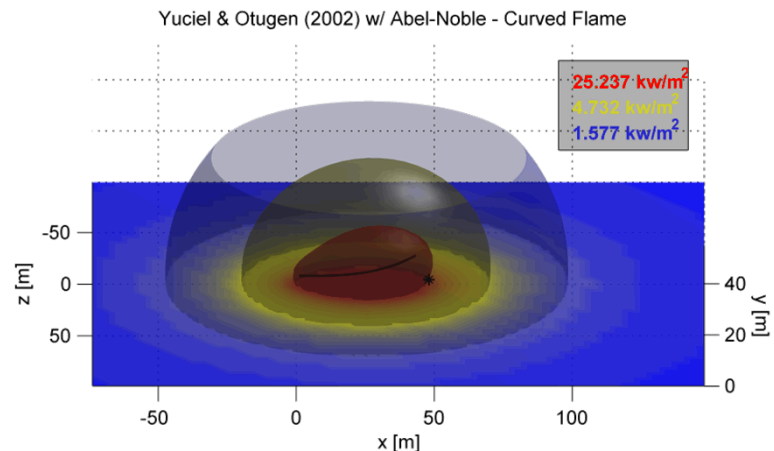
Integral flame model developed to improve downstream H₂ jet flame heat flux prediction.

Ekoto et al. ICHS 2013



Adjusts placement of radiative emitters for new multi-source model – FY12 accomplishment

d_j [mm]	\dot{m} [kg/s]	p_0 [barg]	T_0 [K]	RH	T_{amb} [K]	p_{amb} [mbar]	U_{wind} [m/s]	Wind dir [°]
52.5	7.4	62.1	287.8	94.5	280	1011	0.83	34.0



SNL preferred source model

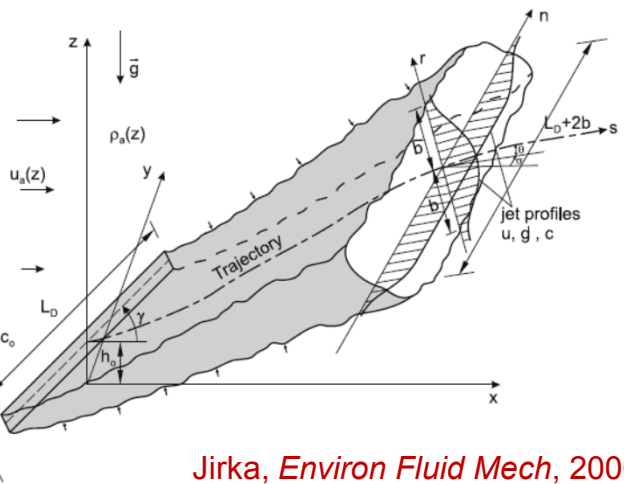
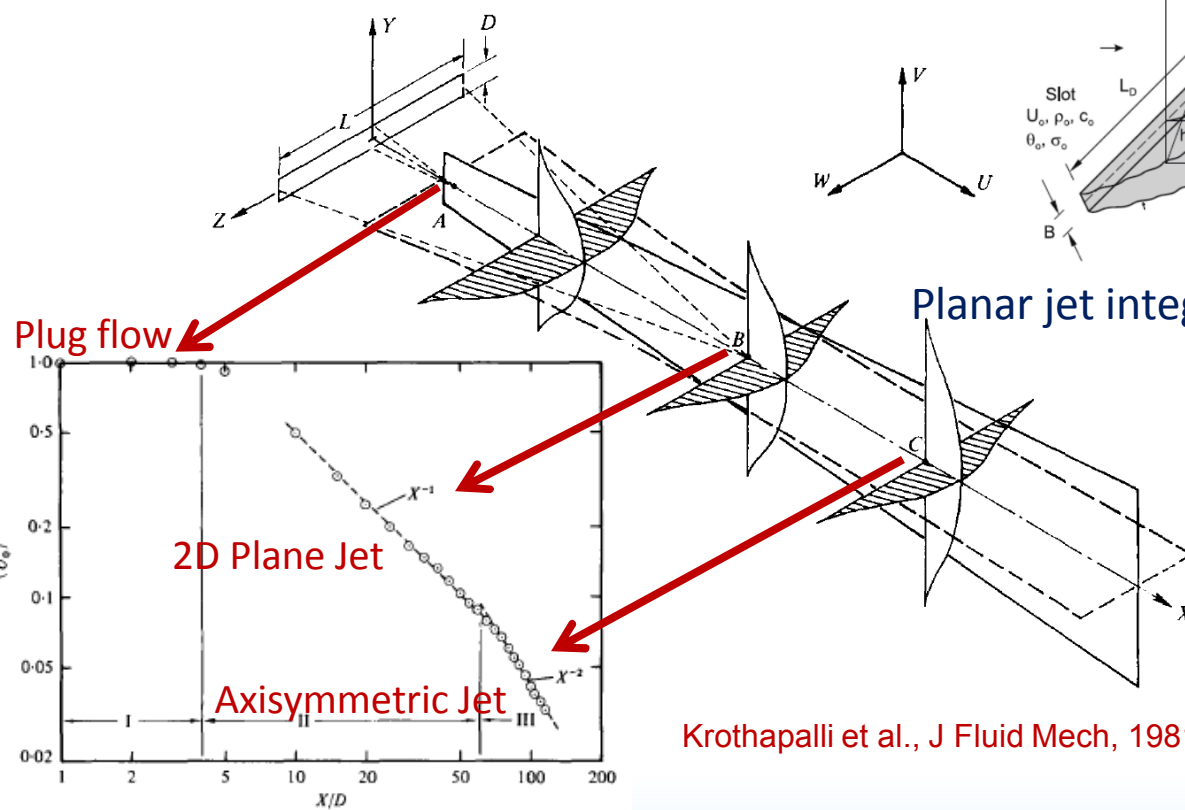


Notional Nozzle Model	L_f [m]	q_{rad} (Straight) [kW/m ²]	q_{rad} (Curved) [kW/m ²]
Measurement	45.9	—	23.9
Birch et al. (1984) w/ Abel-Noble	49.3	97.3	29.9
Yücel & Ötügen (2002) w/ Abel-Noble	44.6	34.8	23.8
Schefer et al. (2007)	44.6	34.8	28.1
Harstad & Bellan (2006) w/ Abel-Noble	52.7	189.8	13.2
Molkov et al. (2009)	49.9	113.2	25.6

Similar wind corrections in progress

Slot Nozzle Modeling

Unchoked slot jets have been thoroughly investigated



Jirka, *Environ Fluid Mech*, 2006

Planar jet integral model has been developed

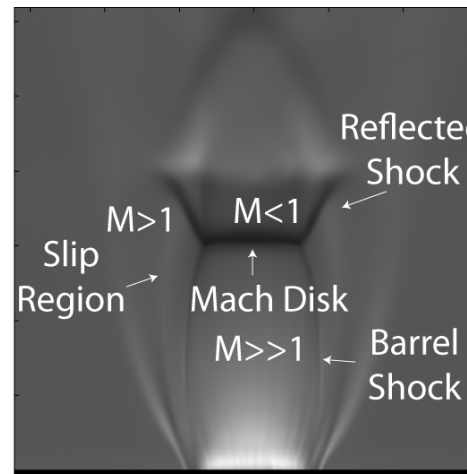
Krothapalli et al., *J Fluid Mech*, 1981

Distinct 2D region with inverse $\frac{1}{2}$ power centerline decay rate exists

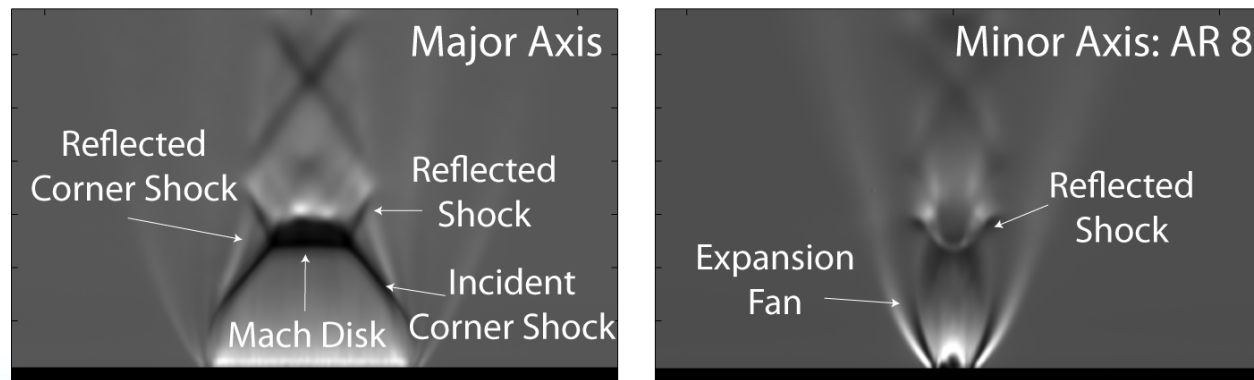
Unclear if models are applicable to choked slot jets

Close-up schlieren imaging reveals unique slot nozzle behavior

– FY13

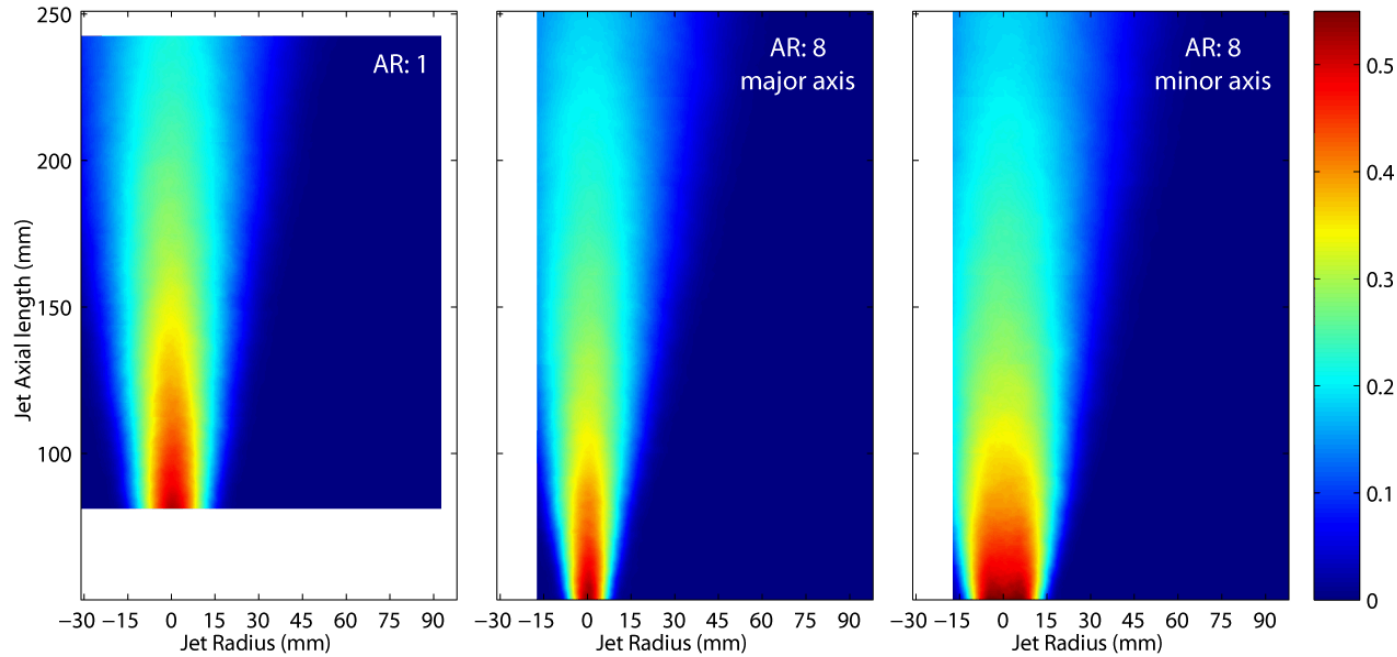


Strong, sharply converging incident corner shock is missing from the minor axis plane



Unclear if existing choked flows notional nozzle models predict correct effective diameters and densities

Mean mass fraction slot jet contours confirm axis switching in the scalar field



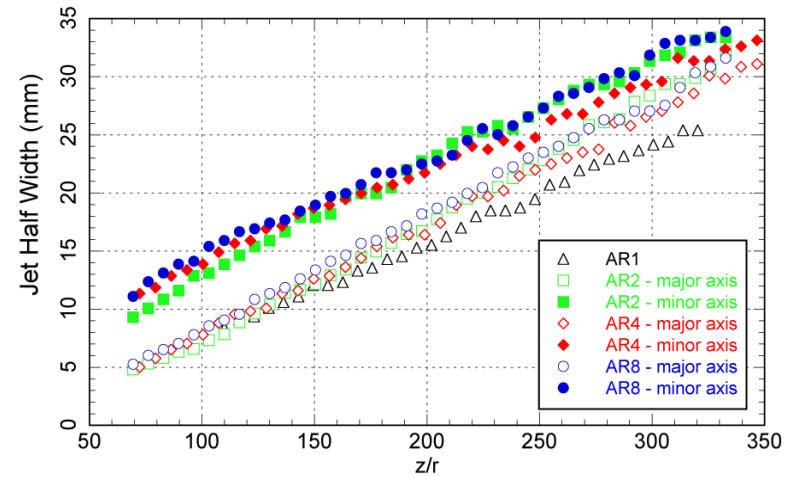
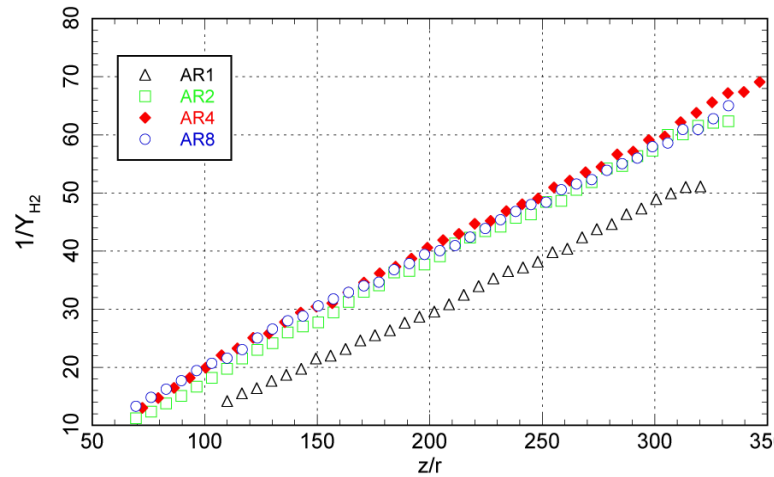
Elevated downstream mass fraction contours for the axisymmetric jet

$$\begin{aligned} D_{eq} &= 1.5 \text{ mm} \\ p_0 &= 10 \text{ bar} \end{aligned}$$

Concentration decay rates remained relatively linear throughout the measurement region

Planar decay region (half-power) not observed

- Upstream of interrogation region?



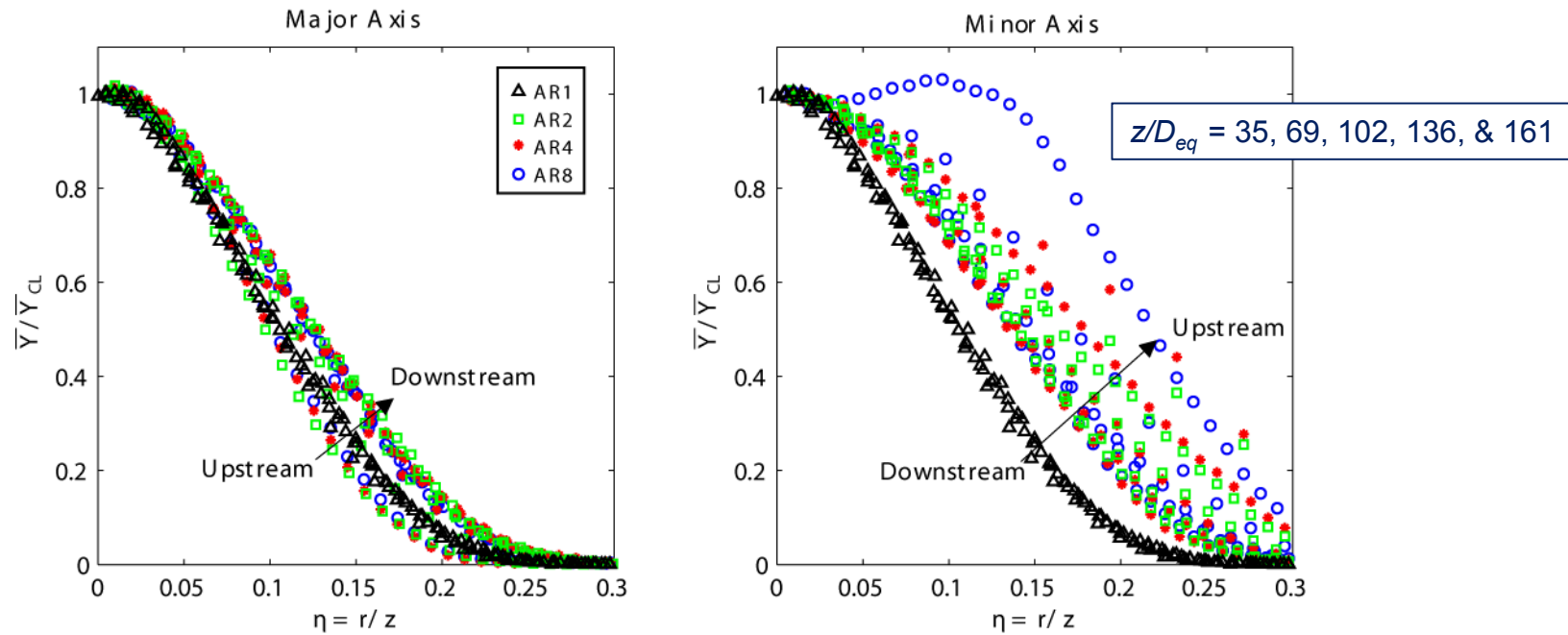
Major & minor axis jet half widths appear to converge

- Half widths larger than for corresponding axisymmetric jet
- Slightly non-linear growth rates – unclear when convergence occurs

Normalized concentration radial profiles along the major/minor axes do not collapse

Axisymmetric profiles collapsed to uniform curves as expected

Normalized profiles grew **wider along the major axis** and **narrower along the minor axis**



Minor axis peak H₂ **near-field** concentrations observed away from the centerline – not predicted by planar integral models

These data will be used to refine jet release characteristics for different release morphologies